

Observations of Global and Regional Ionospheric Irregularities and Scintillation Using GNSS Tracking Networks

Xiaoqing Pi¹, Anthony J. Mannucci¹, Bonnie Valant-Spaight², Yoaz Bar-Sever¹,
Larry J. Romans¹, Susan Skone³, Lawrence Sparks¹, and G. Martin Hall²

¹*Jet Propulsion Laboratory, California Institute of Technology, Pasadena, CA, USA*

²*Propagation Research Associates, Inc., Marietta, GA, USA*

³*University of Calgary, Calgary, Alberta, Canada*

BIOGRAPHY

Xiaoqing Pi, Ph.D, is a Senior Research Technologist at the Jet Propulsion Laboratory, California Institute of Technology. His primary research interests include ionospheric remote sensing and modeling. He has been involved in a number of ionospheric research and system development projects at JPL and is a co-inventor of Global Assimilative Ionospheric Model. Recently he has been a principal investigator of NASA's research projects for imaging the ionosphere using synthetic aperture radar and GPS, and for global mapping of ionospheric irregularities and scintillation using GNSS.

Bonnie Valant-Spaight, Ph.D., is the Head of the Atmospheric Physics Division at Propagation Research Associates, Inc. She performs research on electromagnetic signal propagation in complex environments, including measuring and modeling RF and IR response to refraction and turbulence. Her background includes research in a variety of subjects, including nuclear oil well logging, experimental particle physics, and satellite measurements of the ionosphere. She received her Ph.D. in Physics from Cornell University.

Dr. Yoaz Bar-Sever is a Principal Technologist at JPL, and the Manager of the Global Differential GPS (GDGPS) System.

Larry J. Romans, Ph. D., is a member of the Near Earth Tracking Systems group of the Tracking Systems and Applications section at the Jet Propulsion Laboratory. His interests include various applications of GNSS data, such as real-time orbit determination and remote sensing. He is a co-author and developer of NASA's Global Differential GPS System (GDGPS).

Susan Skone, Ph.D., is an Associate Professor in Geomatics Engineering and Associate Dean (Research), Schulich School of Engineering, at the University of Calgary. She has a background in space physics and conducts research in ionospheric and tropospheric effects on GPS. She has developed software for mitigation of atmospheric effects and leads the GPS payload for CanX-2.

Lawrence Sparks, Ph.D., is a member of the Ionospheric and Atmospheric Remote Sensing Group in the Tracking Systems and Applications Section at NASA's Jet Propulsion Laboratory. He received his Ph.D. in Applied Physics from Cornell University and has pursued research in various fields including fusion plasma physics, solar magnetohydrodynamics, atmospheric radiative transfer, and ionospheric modeling. He is a member of the WAAS Integrity and Performance Panel and is currently working on issues concerning the impact of the ionosphere on satellite-based augmentation systems.

G. Martin Hall, PhD., is a Senior Scientist at Propagation Research Associates, Inc. His primary interest is technology product development. At PRA, he developed an innovative GPS multi-aperture, multi-frequency receiver and signal processing algorithms to measure wave front distortions (angle of arrival) and L1/L2 group delays to determine the state of the troposphere and ionosphere. In addition, he is currently working on an anti-jam GPS receiver based on holographic processing, which enables clutter, multipath, and jamming signals to be separated from the PRN signals and suppressed.

ABSTRACT

The rate of TEC index (ROTI) [1] is a measurement that characterizes ionospheric irregularities. It can be obtained from standard GNSS dual-frequency phase data collected

using a geodetic type of GNSS receiver. By processing GPS data from ground-based networks of International GNSS Service and Continuously Operating Reference Station (CORS), ROTI maps have been produced to observe global and regional scintillation activities. A major mid-latitude scintillation event in the contiguous United States is reported here that was captured in ROTI maps produced using CORS GPS data collected during a space weather storm. The analyses conducted in this work and previously by another group indicate that ROTI is a good occurrence indicator of both amplitude and phase scintillations of GPS L-band signals, even though the magnitudes of ROTI, S_4 , and σ_ϕ can be different. For example, our analysis indicates that prominent ROTI and the L1 phase scintillation (σ_ϕ) are well correlated temporally in the polar region while L1 amplitude scintillation rarely occurs. The differences are partially attributed to physics processes in different latitude regions, such as high-speed plasma convection in the polar region that can suppress the amplitude scintillation. An analysis of the impact of ionospheric scintillation on precise positioning, which requires use of dual-frequency phase data, is also conducted. The results indicate that significant (more than an order of magnitude) positioning errors can occur under phase scintillation conditions.

INTRODUCTION

There exist thousands of dual-frequency geodetic types of GNSS receivers that have been deployed at globally and regionally distributed permanent stations. The networks of such receiver stations include the global GNSS network managed by the International GNSS Service (IGS), the Continuously Operating Reference Station (CORS) network managed by the U.S. National Geodetic Survey, the GPS Earth Observation Network (GEONET) developed by the Geographical Survey Institute of Japan, etc. The standard GNSS data collected from these networks have been used for many scientific and technological applications, including geodetic survey, precise GNSS orbit determination, global differential GPS System, global total electron content (TEC) mapping [2][3], ionospheric irregularity and scintillation measurements, etc.

In this study, we further introduce the rate of TEC index (ROTI) maps that measure global and regional ionospheric irregularity and scintillation activities using the standard dual-frequency GNSS phase data. The measurement technique was originally proposed in 1997 [1]. The coverage of GNSS-inferred ROTI maps has significantly improved since then as the GNSS networks continuously expand. We will show cases of global and regional ionospheric weather variations and space weather effects that are captured in ROTI maps. Results of a correlation analysis will be presented that show ROTI is a good indicator of ionospheric scintillation occurrence

traditionally measured by the S_4 and σ_ϕ indices. Experiments of GNSS-based precise positioning, which require use of dual-frequency phase data, will also be presented that show degradation of positioning accuracy under phase scintillation conditions.

THE RATE OF TEC INDEX

A typical modern geodetic type of GPS receiver is capable of tracking dual-frequency (L1 and L2) GPS signals transmitted up to 12 or 16 GPS satellites simultaneously. GPS phase and pseudorange data are acquired for precise positioning and geodetic survey purposes. Using the dual-frequency phase data, relative total electron content (TEC) and rate of TEC (ROT) change can be measured. The rate of TEC index (ROTI) was originally proposed to measure ionospheric irregularities using GPS data [1]. The index characterizes ROT changes by computing the standard deviation of detrended ROT over a time interval, i.e.,

$$\text{ROTI} = \sqrt{\langle \text{ROT}^2 \rangle - \langle \text{ROT} \rangle^2}. \quad (1)$$

Figure shows an example of ROTI measurements along with the ground projection of GPS PRN17 satellite tracking, observation elevation angle, TEC, and ROT. The measurements were made during May 16, 1995, using a geodetic GPS receiver of the International GNSS Service (IGS) stationed in Yellowknife (62.48°N, 245.52°E), Canada. TEC perturbations and irregularities in relative line-of-sight TEC (labeled as L1-L2 in the figure representing the GPS dual-frequency phase difference), ROT, and ROTI can be clearly identified in this example.

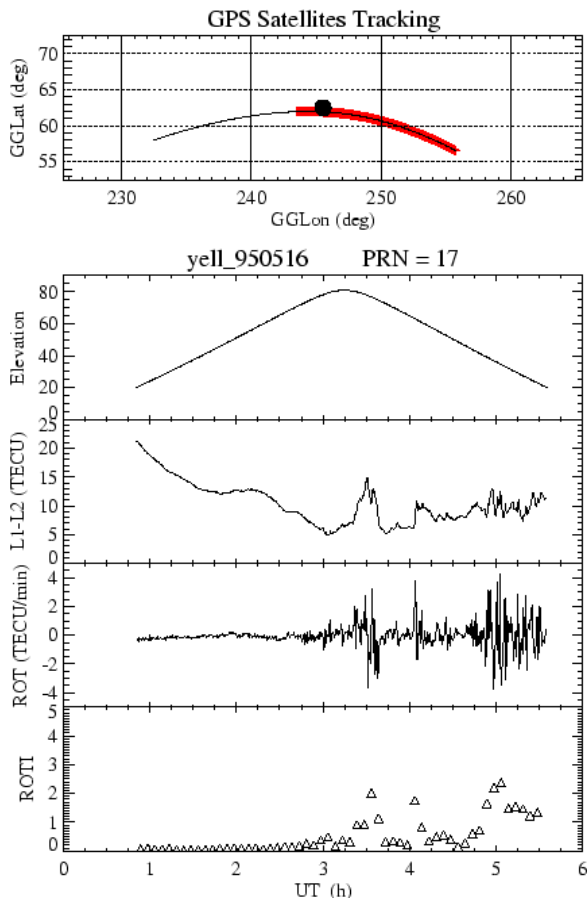


Figure 1. TEC, ROT, and ROTI derived from dual-frequency GPS phase data collected from an IGS site at Yellowknife during May 16, 1995. The projected ground track to the PRN17 satellite and observation elevation angles are also shown. The red color indicates the projected locations of observed ionospheric irregularities.

Compared with specialized scintillation receivers, which provide the standard scintillation indices S_4 and σ_ϕ measurements based on single-frequency signal 50-Hz amplitude and phase data, respectively, a few advantages make the ROTI measurement attractive:

- 1) it can be obtained using data from standard geodetic GNSS receivers that (thousands of them) are already deployed globally;
- 2) it is not susceptible to receiver clock/oscillator error, which can hinder the phase scintillation index σ_ϕ . The dual-frequency data allow removal of the clock error in TEC and ROT measurements;
- 3) it measures directly ionospheric TEC irregularities.

GLOBAL AND REGIONAL ROTI MAPS

The present IGS global GNSS network includes about 427 permanent GNSS Stations. Figure 2 presents the

distribution of a selected subset of these stations. The CORS network in North America managed by the National Geodetic Survey (NGS) is composed of nearly two thousand geodetic receivers (Figure 3). These networks are great assets for measuring space weather effects in the ionosphere, particularly ionospheric irregularities that cause phase and power/amplitude scintillation in radio signals such as the L-band GPS signals. The GNSS receivers installed at these stations are all high quality geodetic types and capable of tracking dual-frequency GNSS signals.

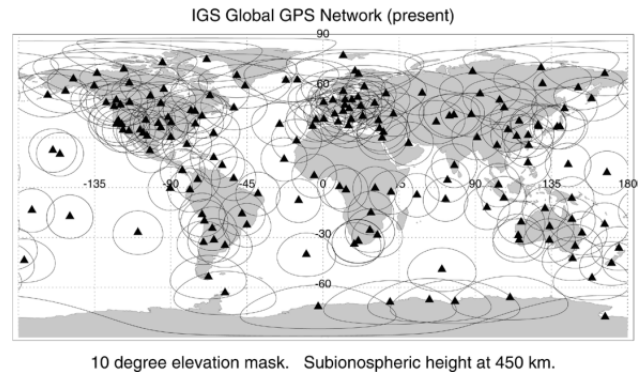


Figure 2. The IGS global GNSS network (selected stations) with observation masks (circles).

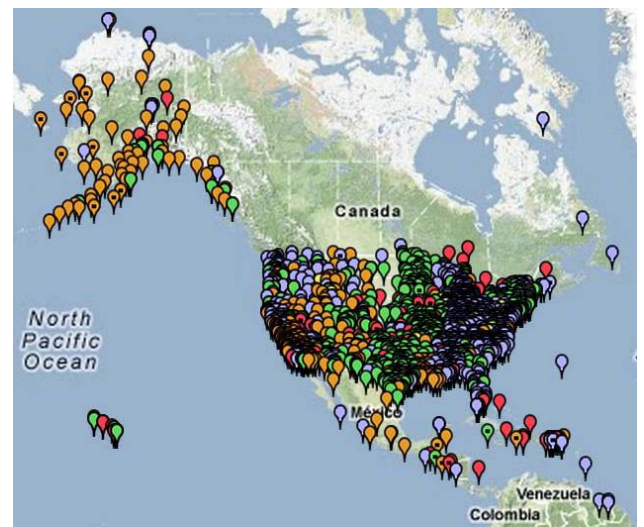


Figure 3. The Continuously Operating Reference Station (CORS) network.

Using standard GPS data collected from the IGS or CORS network, global or regional snapshot ROTI maps can be produced for every 5- to 15-minute intervals. In each global ROTI map, ROTI measurements with corresponding coordinates of 400-km ionospheric piecing points are projected to the ground locations that are binned into 2.5×5 degree pixels (latitude \times longitude). The spatial resolution can be finer if desired. The median

ROTI value in each bin is then obtained to represent irregularity activity in the area. A ROTI map can then be visualized with color coded median ROTI to show the occurrence of ionospheric irregularities and the ROTI strength in the UT interval. Figure 4 shows an example of Global ROTI map (saturated for ROTI > 1 TECU/min) for the 0015-0030 UT interval on March 9, 2012. It is produced using GPS data collected from 441 sites (selected from 1929 stations) of the IGS and CORS networks. A white pixel means no data in the cell. A major geomagnetic storm occurred during this day while the planetary magnetic Ap index reached 87. Intensive irregularity and scintillation activities in both polar regions are captured in the ROTI map besides low-latitude scintillation in a South America region near 45°W longitude around 9 PM local time.

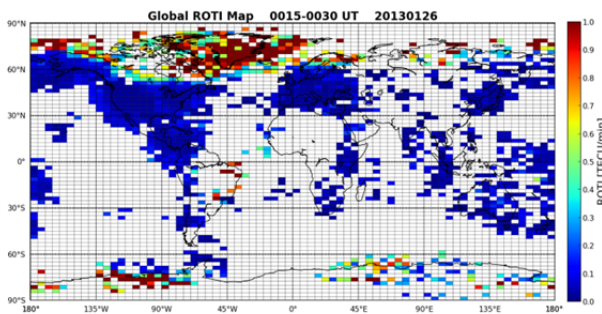


Figure 4. A global ROTI map produced using IGS and CORS GPS data collected on March 9, 2012, when a major geomagnetic storm occurred.

In addition, regional ROTI maps can also be produced with finer spatial resolutions in regions where the distribution of observing sites is relative densely. Figure 5 and 6 show two examples of North America ROTI map snapshots produced using archived CORS GPS data for November 14, 2012, and January 1, 2013. For each of the two examples, GPS data from more than 450 stations are selected from more than 1770 stations to produce ROTI measurements for each site for 24 hours each day. The regional ROTI maps (15-minute UT interval) show the median ROTI values (saturated for ROTI > 1 TECU/min) in 2 × 2 degree pixels (latitude × longitude). The two examples show ROTI maps for the same UT interval (0330 – 0345 UT) but for a storm day (11/14/2012) and quiet day (01/01/2013), respectively. The storm day is identified by geomagnetic 3-hour Kp (6+ for this interval) and daily Ap (= 37) indices, while Kp index on the quiet day is about 0 to 1.

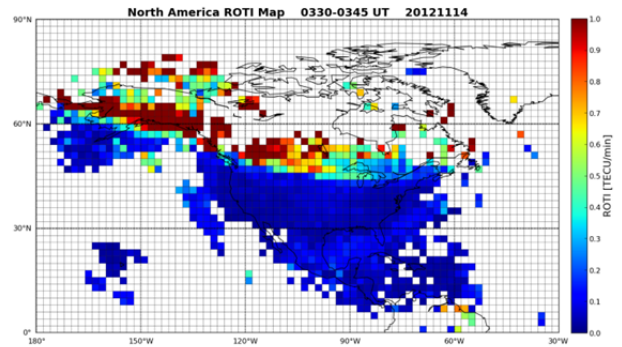


Figure 5. North America ROTI maps produced using GPS data collected from the CORS network for 0330 – 0345 UT interval on a storm day (November 14, 2012).

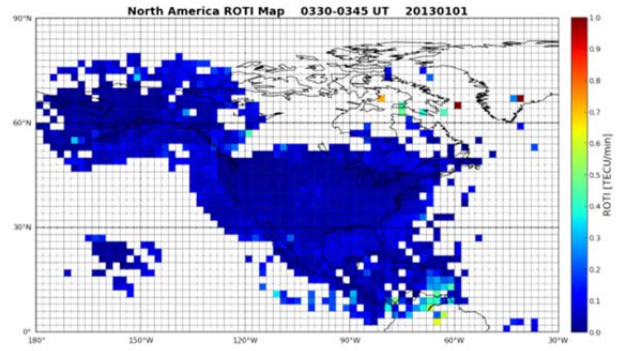


Figure 6. North America ROTI maps produced using GPS data collected from the CORS network for 0330 – 0345 UT interval on a quiet day (January 1, 2013).

On the storm day, the North America ROTI map shows that ionospheric irregularities, which cause GPS signal phase scintillation, occurred not only in the polar region particularly in Alaska and Canada but also expanded down to the mid-latitude region in the northern part of the United States near the Canadian border. In addition, low-latitude irregularities or scintillation can also be seen near the equator. On the quiet day, we do not see ionospheric irregularities in the entire polar and middle latitude regions, except for a few isolated spots. However, the quiet-time ROTI map indicates irregularity and scintillation activity at low latitudes near 65°W longitude sector. The low-latitude scintillation activity during a geomagnetically quiet day is driven by the low-latitude aeronomy rather than solar-magnetospheric events.

In fact, during severe geomagnetic storms, ionospheric irregularity and scintillation activity in the polar region can expand to lower latitudes in the Contiguous United States (CONUS). Such an event occurred during April 6, 2000, and the CORS network captured major disturbances. During this day, the planetary magnetic Ap index reached 82, and Kp indices during 19 – 24 UT reached 8+. Figure 7 shows a couple of examples of ROTI maps produced for this day using GPS data collected from 178 CORS receivers. During 2100 – 2400

UT, ionospheric irregularities measured by ROTI can be seen in large (if not most) areas of the CONUS region, as shown in the examples.

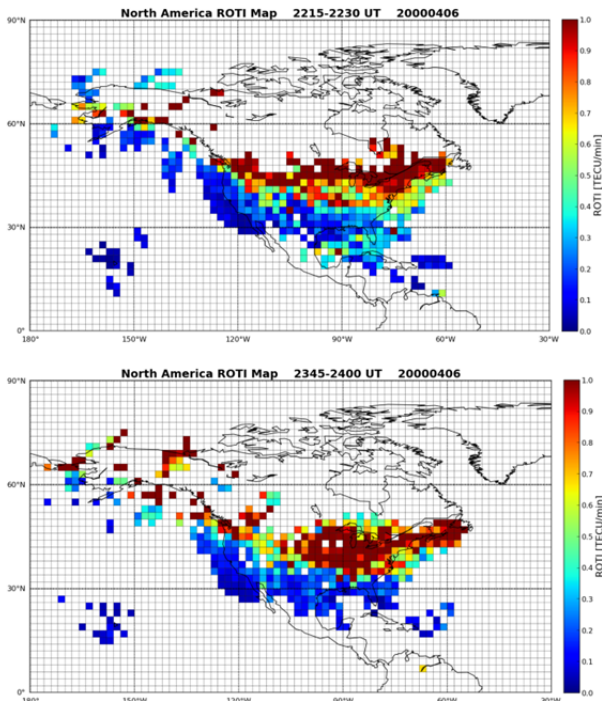


Figure 7. North America ROTI maps for the 2215 – 2230 UT and 2345 – 2400 UT intervals during April 4, 2000, when a severe geomagnetic storm occurred.

The above four examples show that ROTI maps capture ionospheric irregularity and scintillation activity very well during either disturbed or quiet period. Such ROTI maps can be produced continuously in real time if real-time data is accessible. Real-time ROTI maps can serve the monitoring of ionospheric irregularities and scintillation under various space and ionospheric weather conditions.

CORRELATION BETWEEN ROTI AND SCINTILLATION INDICES S_4 AND σ_ϕ

With ROTI measurements, one question is often raised: Is ROTI correlated with other scintillation measurements such as S_4 and σ_ϕ ? Beach and Kintner [2] conducted a study to assess the correlation between ROTI and S_4 based on GPS measurements made from an equatorial site in South America. Their conclusion is that ROTI obtained from 30-second sampled data does fairly well in tracking scintillation periods identified using S_4 measurements, though the spectral information contained in 50-Hz data is missing that could help to improve the quality of predicting S_4 . Figure 8 shows an example of their observations. In their study, analysis of correlation between ROTI and phase scintillation measurement σ_ϕ

was not included, probably due to the lack of quality phase measurements by the receiver.

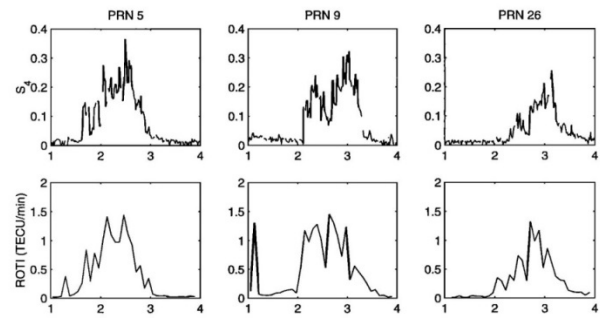


Figure 8. ROTI and S_4 comparison made using GPS data collected from Ancon, Peru. The horizontal scale is UT in hours. [Beach and Kintner, 1999; courtesy of the American Geophysical Union.]

To measure space weather effects in the ionosphere and mitigate the impact of the effects on GPS and other radio technology users in regions such as North America, scintillation characteristics in the polar and sub-auroral regions must be addressed. Under geomagnetic storm conditions, the ionosphere becomes highly structured in the polar region, and the plasma convection speeds can reach ~ 1 to 2 km/s, an order of magnitude higher than plasma drift speeds at low latitudes (~ 100 m/s). The high-speed convection plays a role to suppress amplitude scintillation due to the Fresnel filtering effect [3], while phase scintillation remains strong. This type of activity can expand to the sub-auroral middle-latitude region under certain storm conditions (as shown in the next section).

To examine ROTI, σ_ϕ , and S_4 measurements in the polar region, we analyzed GPS L1 scintillation data (σ_ϕ and S_4) and ROTI data from a receiver located at Yellowknife, Canada. This GPS scintillation receiver tracked the L1 and L2 dual-frequency signals and measured L1 σ_ϕ and S_4 . Prof. Susan Skone from the University of Calgary, Canada provided L1 scintillation and ROT data collected during 24 hours on August 26 and October 3, 2005. The ROT, and L1 σ_ϕ and S_4 data are sampled at 1-minute intervals, but ROT in each minute is computed for several different data cadences, including 30 seconds. ROT computed for 30-second cadence is chosen for this analysis since most of the geodetic data archives of the IGS and CORS networks adopt this sampling rate (some receivers also collect data at 1 Hz rate).

Examining the ROTI, σ_ϕ and S_4 data, we find the following characteristics:

- 1) Phase scintillation (σ_ϕ) frequently occurs during the two days while amplitude scintillation (S_4) rarely occurs.

- 2) Phase scintillation is very well correlated with the occurrence of prominent ROT changes.
- 3) Prominent ROT changes and phase scintillation are well associated with rapid irregular TEC variations or structures seen in TEC data directly.

A couple of examples of TEC, ROT, σ_ϕ , and S_4 data are given in Figure 9 showing the correlation between ROT and phase scintillation data. In fact, these are typical cases that are seen in the GPS data throughout these two days.

In addition to examining temporal correlation, we have also performed an analysis to compare the magnitudes of ROTI and σ_ϕ over the same intervals. In this analysis, ROTI value and mean σ_ϕ are computed for the same intervals. The computed ROTI and mean σ_ϕ values are then compared. Figure 10 shows a comparison of ROTI obtained with 15 ROT samples and 15-minute averaged σ_ϕ ($\langle \sigma_\phi \rangle$). The plot includes all measurements of the two days (outliers and excessively noisy data are removed). The comparison shows although ROTI tracks phase scintillation occurrence very well, the magnitude of ROTI and $\langle \sigma_\phi \rangle$ does not exactly follow a linear relationship, and the correlation coefficient of their magnitude is about 0.763 for the data sets of the two days.

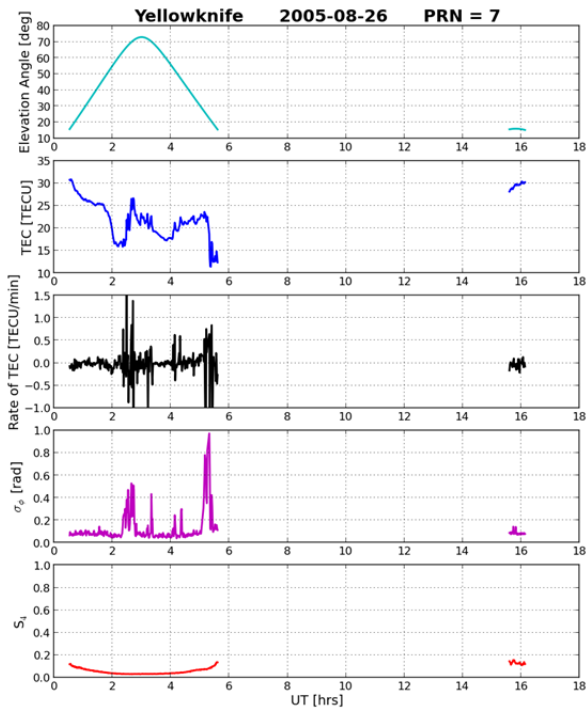


Figure 9(a). TEC, ROT, σ_ϕ (GPS L1 phase scintillation), and S_4 (GPS L1 amplitude scintillation) measured using a GPS receiver tracking GPS PRN7 and PRN10 satellites, respectively, from Yellowknife, Canada, during August 26, 2005. The measurements shows well correlated ROT changes and phase scintillation and they were associated with irregular TEC variations, while amplitude scintillation did not occur.

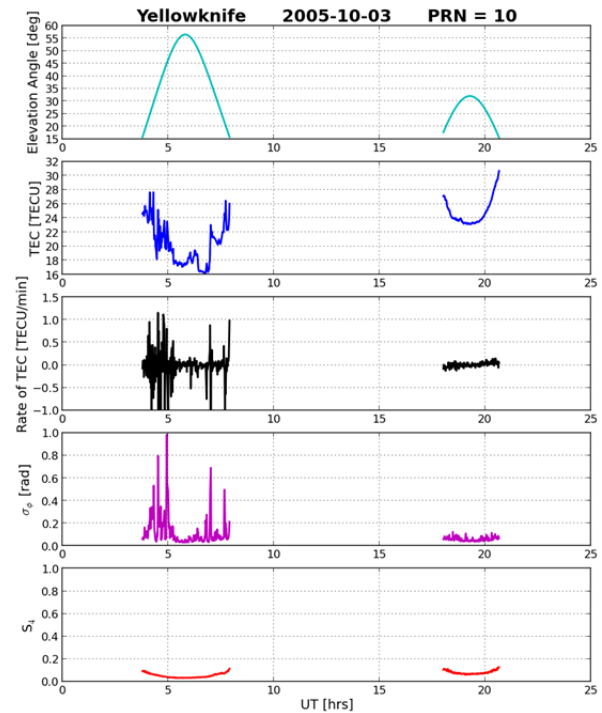


Figure 9(b). Similar as Figure 9(a) for October 3, 2005.

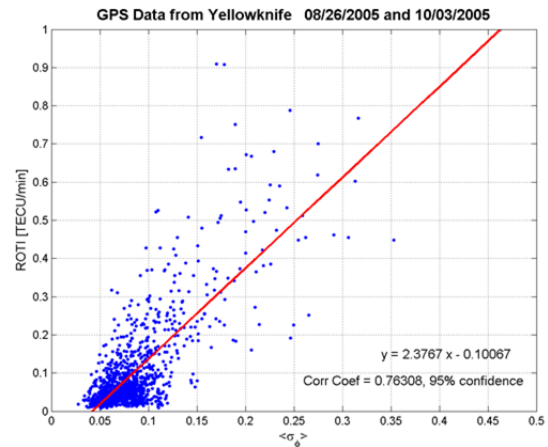


Figure 10. Comparison of ROTI and $\langle \sigma_\phi \rangle$ derived from GPS data collected from Yellowknife, Canada, during August 26 and October 3, 2005.

To understand the differences between ROTI and σ_ϕ , we consider the following factors. The σ_ϕ index measures 50-Hz phase fluctuations around the mean phase for the time interval (1 minute). On the other hand, TEC, ROT and ROTI are based on the decimated 30-second phase data. The fact that the occurrence of prominent ROT changes or ROTI and phase scintillation is well correlated indicates that the observed phase scintillation is caused by ionospheric irregularities measured by ROTI. The difference in their magnitude can be attributed to the fact that the phase scintillation index is affected not only by

electron density fluctuations but also by other factors, such as irregularity spectrum, observation geometry, radio wavelength, speed of plasma, etc. In fact, the magnitude of S_4 and σ_ϕ does not follow a linear relationship either. Nevertheless, ROTI is a good indicator of phase scintillation at high and sub-auroral latitudes, and of both amplitude and phase scintillation at low latitudes, even though the magnitudes of ROTI, σ_ϕ , and S_4 show differences.

IMPACT OF IONOSPHERIC SCINTILLATION ON PRECISE POSITIONING

In this section, we report an analysis of the impact of ionospheric scintillation on precise positioning. Our positioning experiments are conducted using the GNSS Inferred Positioning System and Orbit Analysis Simulation Software (GIPSY-OASIS, briefly GIPSY, <https://gipsy-oasis.jpl.nasa.gov/>) developed at the Jet Propulsion Laboratory. The GIPSY takes corrected GPS satellite orbit and clock data (also obtained using GIPSY) as well as user's dual-frequency GNSS phase and pseudorange data to determine the user position. The phase data is used to smooth the pseudorange data to reduce the multipath noise/error, while the dual-frequency data is used to remove the signal time delay induced by the ionosphere. In addition, GIPSY includes intensive data editing processes to remove data outliers and reduce data noise. Under nominal conditions, the accuracy of post-processed positioning using GIPSY is at a few centimeter level (standard deviation).

Our analysis is performed in the context of space weather effect and quiet conditions during November 14, 2012, and January 1, 2013 as shown in Figures 5 and 6, respectively, described in the previous section. We applied GIPSY to the GPS data collected during the scintillation and quiet day, respectively. For both days, same three sites are selected for the positioning experiments: AB39 (66.559°N, 214.787°E), AC31 (64.638°N, 197.761°E), and AC50 (65.554°N, 195.433°E), and all sites are located in the polar region. Figures 11(a), 7(b), and 7(c) show the number of GPS satellites in view, number of scintillating links (ROTI > 0.5 TRCU/min), <ROTI> averaged over all observations, and position deviations from the nominal positions of these sites for every 5 minutes throughout 24 hours. The position deviations are measured in x, y, and z coordinates in the Earth Centered Earth Fixed (ECEF) coordinate system. It is noticed that at all three sites, there are periods of increased or large positioning errors during scintillation hours. These errors can exceed 1 meter, which is about 20 to 50 times larger than the centimeter level accuracy. As a contrast, on the quiet day the positioning throughout 24 hours at these sites does not show large deviations or jumps (Figure 12) as seen in the days with scintillation present.

To compare statistics of precise positioning errors for the quiet day and scintillation day, Table 1 is given that summarizes the standard deviation of differences between estimated coordinates and the provided (fixed) location coordinates for the two days.

These two experiments indicate that even with state-of-the-art precise positioning techniques, significant positioning degradation can occur under phase scintillation conditions. It should also be noted that our experiments are conducted in a post processing mode, which allows advanced techniques to reduce data noise and to enhance the positioning performance. In real-time scenarios, positioning techniques are constrained by limited data and processing techniques. We expect that the impact of scintillation on real-time positioning applications is significantly worse than the results seen in our experiments.

Table 1. Daily Statistics of Positioning Error

	CORS Site	σ_x (m)	σ_y (m)	σ_z (m)
01/01/2013 (Quiet)	AB39	0.023	0.021	0.053
	AC31	0.043	0.038	0.066
	AC50	0.041	0.037	0.062
11/14/2012 (Scintillation)	AB39	0.087	0.117	0.257
	AC31	0.140	0.126	0.126
	AC50	0.195	0.163	0.539

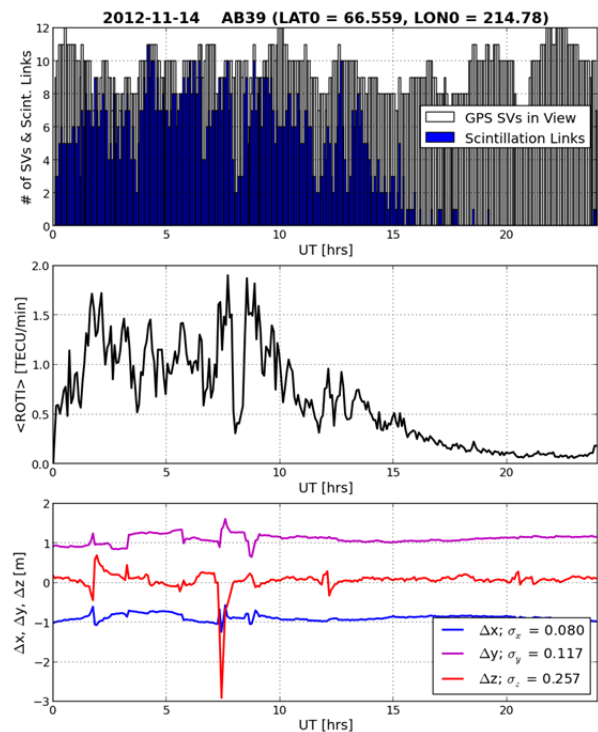


Figure 11(a). Plotted are the deviations of GPS-determined position from the provided nominal station location (bottom

panel) measured in x, y, and z coordinates (in the ECEF coordinate system) at a 5-minute cadence during 24 hours on November 14, 2012, for the AB39 station. The number of GPS satellites in view, number of scintillating links where $ROTI > 0.5$ TECU/min, and $\langle ROTI \rangle$ averaged over all observations are also provided as references of GPS observation and ionospheric irregularity/phase-scintillation conditions.

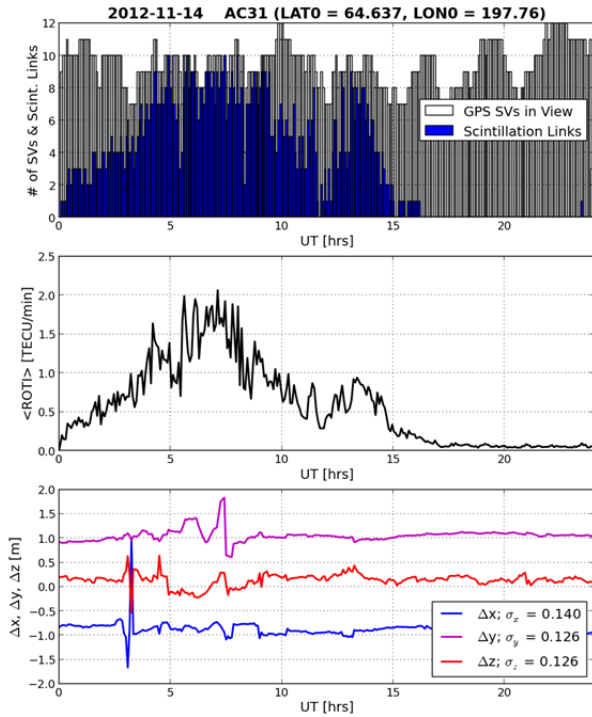


Figure 11(b). Similar plot as Figure 11(a) for the CORS station AC31.

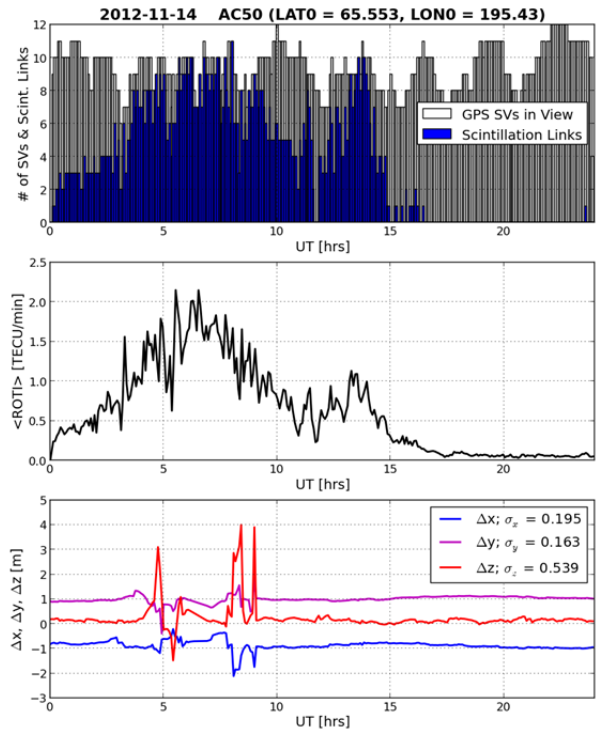


Figure 11(c). Similar plot as Figure 11(a) for the CORS station AC50.

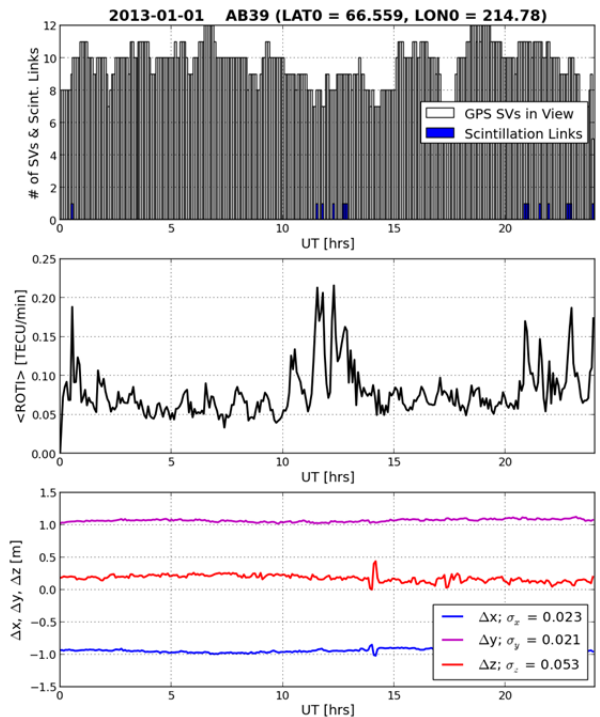


Figure 12(a). Plotted are the deviations of GPS-determined position from the provided nominal station location (bottom panel) measured in x, y, and z coordinates (in the ECEF coordinate system) at a 5-minute cadence during 24 hours on January 1, 2013, for the CORS AB39 station. The number

of GPS satellites in view, number of scintillating links where ROTI > 0.5 TECU/min, and <ROTI> averaged over all observations are also provided as references of GPS observation and ionospheric irregularity/phase-scintillation conditions.

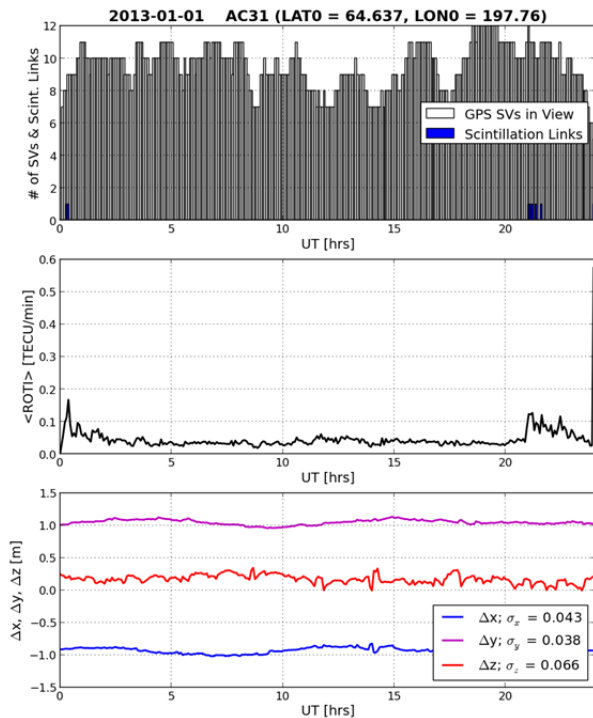


Figure 12(b). Similar plot as Figure 12(a) for the CORS station AC31.

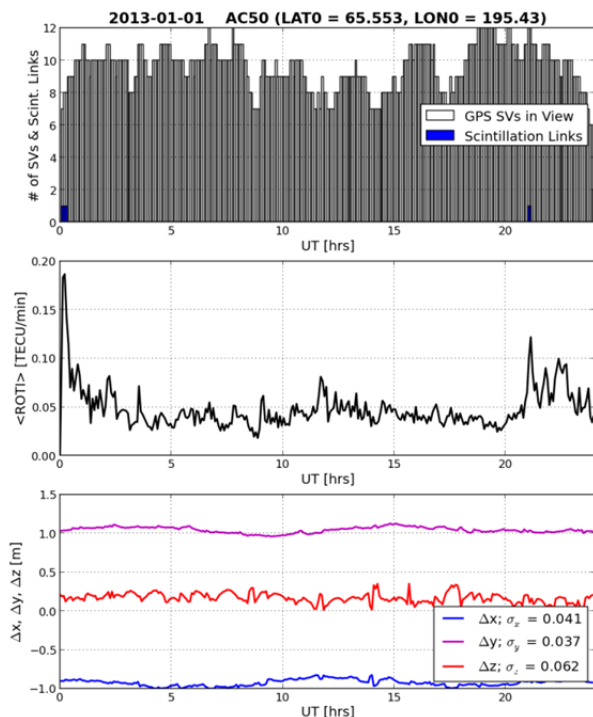


Figure 12(c). Similar plot as Figure 12(a) for the CORS station AC50.

CONCLUSIONS

This study shows that the ROTI measurements obtained using standard GNSS dual-frequency phase data can be used to characterize ionospheric irregularities and scintillation. The presented ionospheric events show that ROTI maps can be used to measure and monitor ionospheric irregularity and scintillation activities globally and regionally under disturbed space weather conditions. A major mid-latitude scintillation event in large areas of the contiguous United States is reported here, which was captured in ROTI maps produced using CORS GNSS data during a severe space weather storm during April 6, 2000.

The correlation analysis conducted in this study indicates that ROTI is a good occurrence indicator of L-band ionospheric scintillation that is measured by the traditional S_4 and σ_ϕ indices. Our analysis also shows that the magnitudes of ROTI, S_4 , and σ_ϕ indices can be different. They do not follow simple linear relations. The differences are partially attributed to the physics processes in different latitude regions. For example, the high-speed plasma convection in the polar region can play a role to suppress L-band amplitude scintillation through the Fresnel filtering effect [3] while phase scintillation (σ_ϕ) and rate of TEC changes (ROTI) remain strong. Our experiments of precise positioning, which require use of dual-frequency phase data, show degradation of positioning accuracy under phase scintillation conditions during space weather events. The degradation can be more than an order of magnitude and expected to be worse in real-time applications, which are constrained by limited data access and processing techniques.

ACKNOWLEDGMENTS

The research conducted at the Jet Propulsion Laboratory, California Institute of Technology, is under a contract with NASA. This work is partially supported by NASA's Heliosphysics Data Enhancement Environments program, FAA's WAAS program, and NOAA's Small Business Innovative Research program.

REFERENCES

- [1] Pi, X., A. J. Mannucci, U. J. Lindqwister, and C. M. Ho, Monitoring of global ionospheric irregularities using the worldwide GPS network, *Geophys. Res. Lett.*, 24, 2283, 1997.
- [2] Mannucci A. J., B. D. Wilson, D. N. Yuan, C. M. Ho, U. J Lindqwister, and T. F. Runge, A global mapping

technique for GPS-derived ionospheric total electron content measurements, *Radio Sci.*, 33(3), 565-583, 1998.

- [3] Iijima, B. A., I. L. Harris, C. M. Ho, U. J. Lindqwister, A. J. Mannucci, X. Pi, M. J. Reyes, L. C. Sparks, and B. D. Wilson, Automated daily process for global ionospheric total electron content maps and satellite ocean altimeter ionospheric calibration based on Global Positioning System data, *J. Atmos. Solar-Terr. Phys.*, 61(16), 1205-1218, 1999.
- [4] Beach, T. L., and P. M. Kintner, Simultaneous Global Positioning System observations of equatorial scintillations and total electron content fluctuations, *J. Geophys. Res.*, 104, A10, pp. 22,553-22,565, 1999.
- [5] Pi, X., B. M. Boulat, B. J. Iijima, A. J. Mannucci, and D. A. Stowers, Latitudinal characteristics of L-band ionospheric scintillation, ION-GPS, Portland, Oregon, September 2002.